

# ELECTRONIC SUPPORTING INFORMATION

## Controlled Radical Release with Iron Oxide Nanoparticles Grafted with Thermosensitive Alkoxyamines Triggered by External *Stimuli*

Farah Abdel Sater,<sup>a‡</sup> Basile Bouvet,<sup>a‡</sup> Saad Sene,<sup>a</sup> Gautier Félix,<sup>a</sup> Erwan Adriaenssens,<sup>b</sup> Jean-Patrick Joly,<sup>b</sup> Gerard Audran,<sup>\*b</sup> Sylvain R. A. Marque,<sup>\*b</sup> Joulia Larionova<sup>\*a</sup> and Yannick Guari<sup>a</sup>

<sup>a</sup> ICGM, Univ. Montpellier, CNRS, ENSCM, CNRS Montpellier, France, E-mail : [basile.bouvet@umontpellier.fr](mailto:basile.bouvet@umontpellier.fr) (B.B.) ; [saad.sene@umontpellier.fr](mailto:saad.sene@umontpellier.fr) (S.S.); [gautier.felix@umontpellier.fr](mailto:gautier.felix@umontpellier.fr) (G.F.); [joulia.larionova@umontpellier.fr](mailto:joulia.larionova@umontpellier.fr) (J.L.); [yannick.guari@umontpellier.fr](mailto:yannick.guari@umontpellier.fr) (Y.G.)

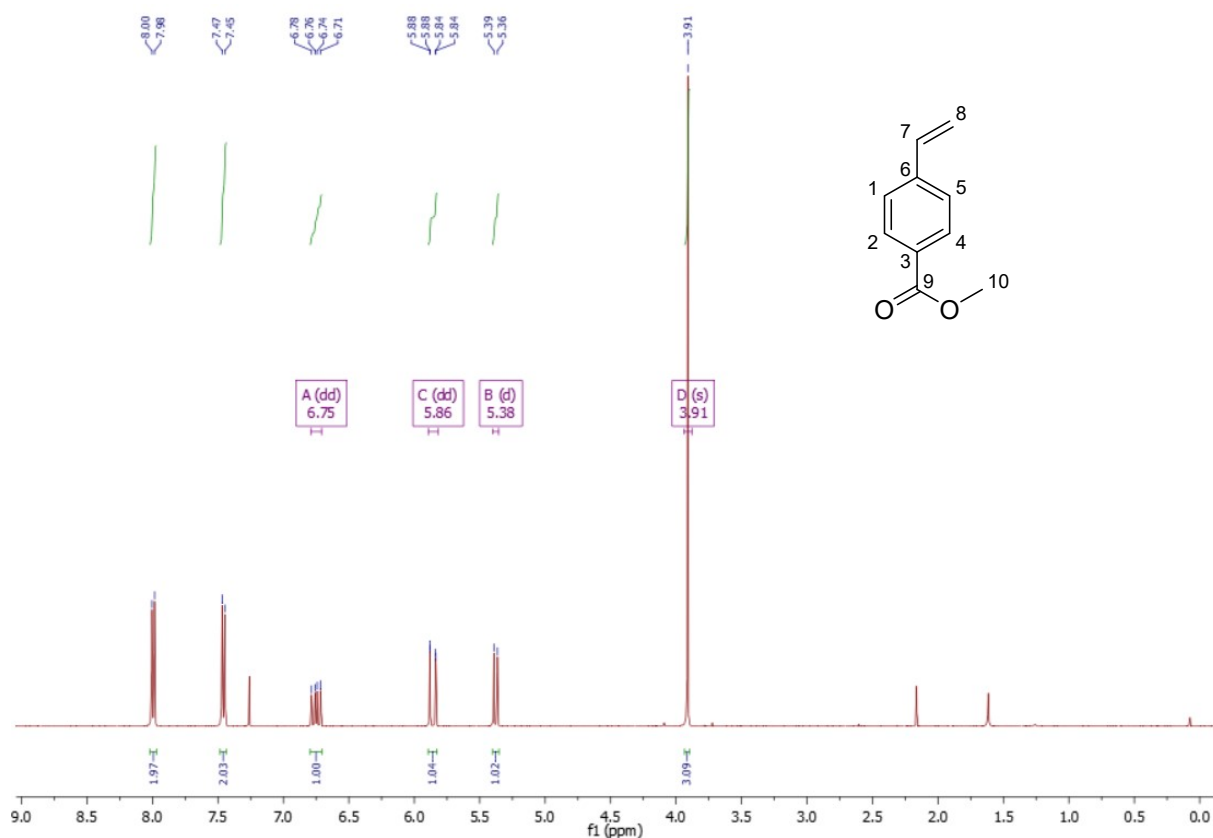
<sup>b</sup> Aix Marseille Univ, CNRS, ICR, UMR 7273, Avenue Escadrille Normandie-Niemen, 13397 Marseille CEDEX 20, France. E-mail : [erwan.adriaenssens@univ-amu.fr](mailto:erwan.adriaenssens@univ-amu.fr), (E.A.) [g.audran@univ-amu.fr](mailto:g.audran@univ-amu.fr), (G.A.) [sylvain.marque@univ-amu.fr](mailto:sylvain.marque@univ-amu.fr) (S.M.)

### Table of Contents

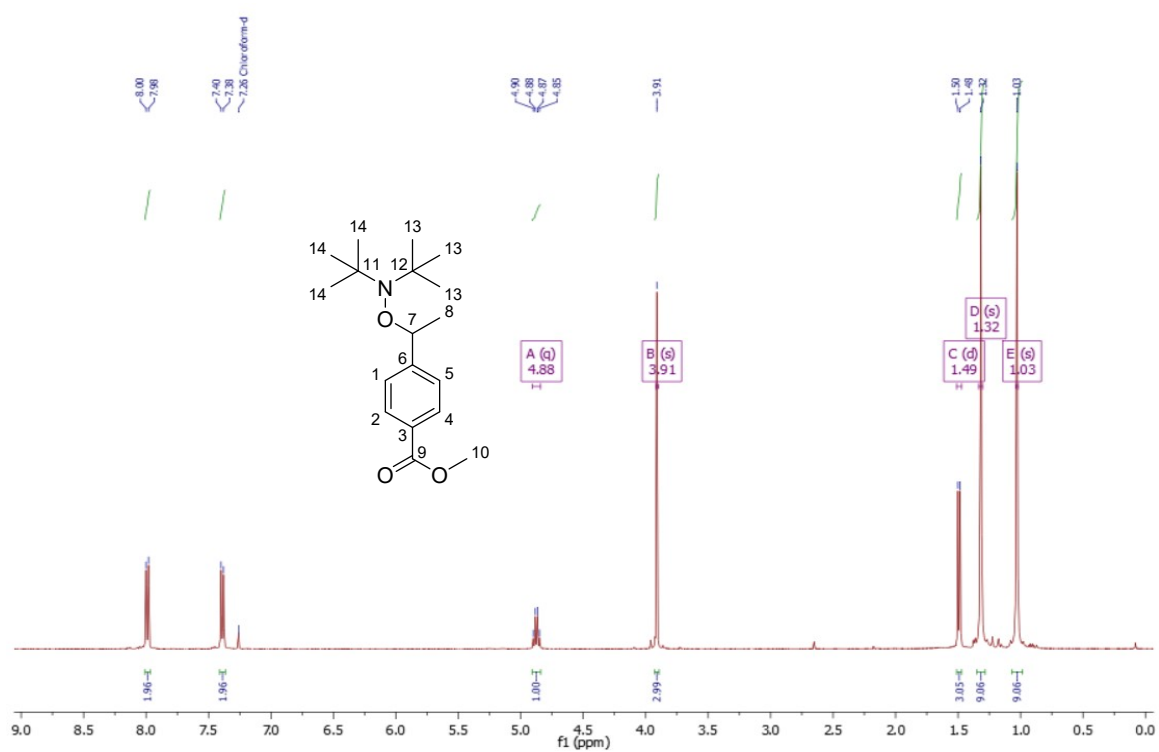
<b>Figures</b> .....	3
<b>Figure S1.</b> <sup>1</sup> H NMR spectrum of Methyl 4-vinylbenzoate. ....	3
<b>Figure S2.</b> <sup>1</sup> H (up) and <sup>13</sup> C (down) NMR spectra of Methyl 4-(1-((di-tert-butylamino)oxy)ethyl)benzoate .....	4
<b>Figure S3.</b> <sup>1</sup> H (up) and <sup>13</sup> C (down) NMR spectra of 4-(1-((di-tert-butylamino)oxy)ethyl)benzoic acid. ....	5
<b>Figure S4.</b> <sup>1</sup> H (up), <sup>13</sup> C (middle) and <sup>31</sup> P (down) NMR spectra of Diethyl (6-(4-(1-((di-tert-butylamino)oxy)ethyl) benzamido) hexyl)phosphonate. ....	6
<b>Figure S5.</b> <sup>1</sup> H (up), <sup>13</sup> C (middle) and <sup>31</sup> P (down) NMR spectra of (6-(4-(1-((di-tert-butylamino)oxy)ethyl)benzamido)hexyl) phosphonic acid .....	8
<b>Figure S6.</b> Histograms showing the size distributions for: (a) IONP/OA/OL nanoparticles, and (b) IONP@alkoxyamine nanoparticles. The standard normal distribution is represented by the red line.....	9
<b>Figure S7.</b> Hydrodynamic diameter distribution by intensity (a) and by number (b) for IONP/OA/OA (in red) and IONP@alkoxyamine (in grey) in methanol. ....	9
<b>Figure S8.</b> Infrared spectra for the pristine IONP (in red), IONP@alkoxyamine (in grey), and free alkoxyamine molecule, ((6-(4-(1-((di-tert-butylamino)oxy)ethyl) benzamido)hexyl)phosphonic acid) (in blue). ....	10
<b>Figure S9.</b> XRD pattern of naked IONP (red) and IONP@alkoxyamine (black) powder and reference diffraction peaks corresponding to Fe <sub>3</sub> O <sub>4</sub> .....	10

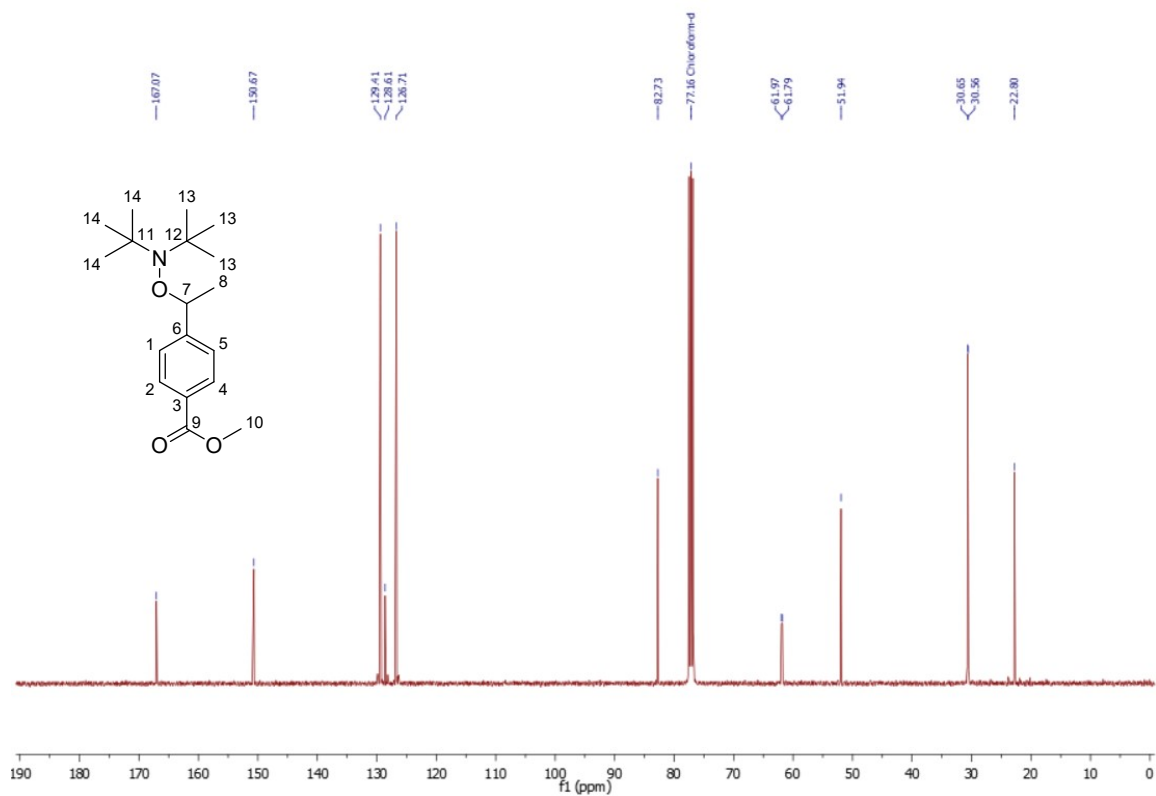
<b>Figure S10.</b> (a) Hysteresis loops performed for the pristine IONP (red squares) and IONP@alkoxyamine nanoparticles (black squares) at 300 K between -6 and 6 T. Temperature dependence of the magnetization performed in the FC (open symbols)-ZFC mode (full symbols) for the pristine IONP (b) and for IONP@alkoxyamine nanoparticles (c) measured under an applied dc magnetic field of 100 Oe. ....	11
<b>Figure S11.</b> a) Magnetothermia experiments performed for IONP@alkoxyamine colloidal solution of 2.9 mg mL <sup>-1</sup> in tert-butylbenzene under different AMF (340 kHz), b) $\Delta T$ vs magnetic field for IONP@alkoxyamine colloidal solution of 2.9 mg mL <sup>-1</sup> in tert-butylbenzene. ....	12
<b>Figure S12.</b> Hydrodynamic diameter distribution by number for IONP@alkoxyamine in a series of solvents 10 min (a) and 2h (b) after dispersion. ....	13
<b>Figure S13.</b> a) The $k_d$ constant as a function of temperature (a) and time (b) used in numerical simulations for IONP@alkoxyamine nanoparticles'homolysis.....	13
<b>Figure S14.</b> EPR spectrum of free alkoxyamine molecule in tert-butylbenzene submitted to laser irradiation at 808 nm (laser power of 2.6 W.cm <sup>-2</sup> ) during 20 minutes.....	14
<b>Figure S15.</b> (a) EPR spectra for the <i>tert</i> -butylbenzene solutions of IONP@alkoxyamine (2.9 mg.mL <sup>-1</sup> ) before and after 10, 20 and 40 min after light irradiation at 808 nm (2.6 W.cm <sup>-2</sup> ); (b) Homolysis kinetic represented as $C/C_0$ vs time curve. The red line represents the best fit with the eq. (1): $k_d = 3.6 \cdot 10^{-2} \text{ s}^{-1}$ , $T_{\text{max}} = 109 \pm 6.7 \text{ }^\circ\text{C}$ , macroscopic temperature is of 50 $^\circ\text{C}$ . ....	15
<b>Models &amp; theory</b> .....	16
<b>1. Determination of the Specific Absorption Rate (SAR)</b> .....	16
<b>2. Fits for the <math>\Delta T</math> as a function of the concentration curve for magneto- and photothermia experiment</b> .....	17
<b>3. Investigation of the homolysis kinetic of the radical release by EPR</b> .....	18

# Figures

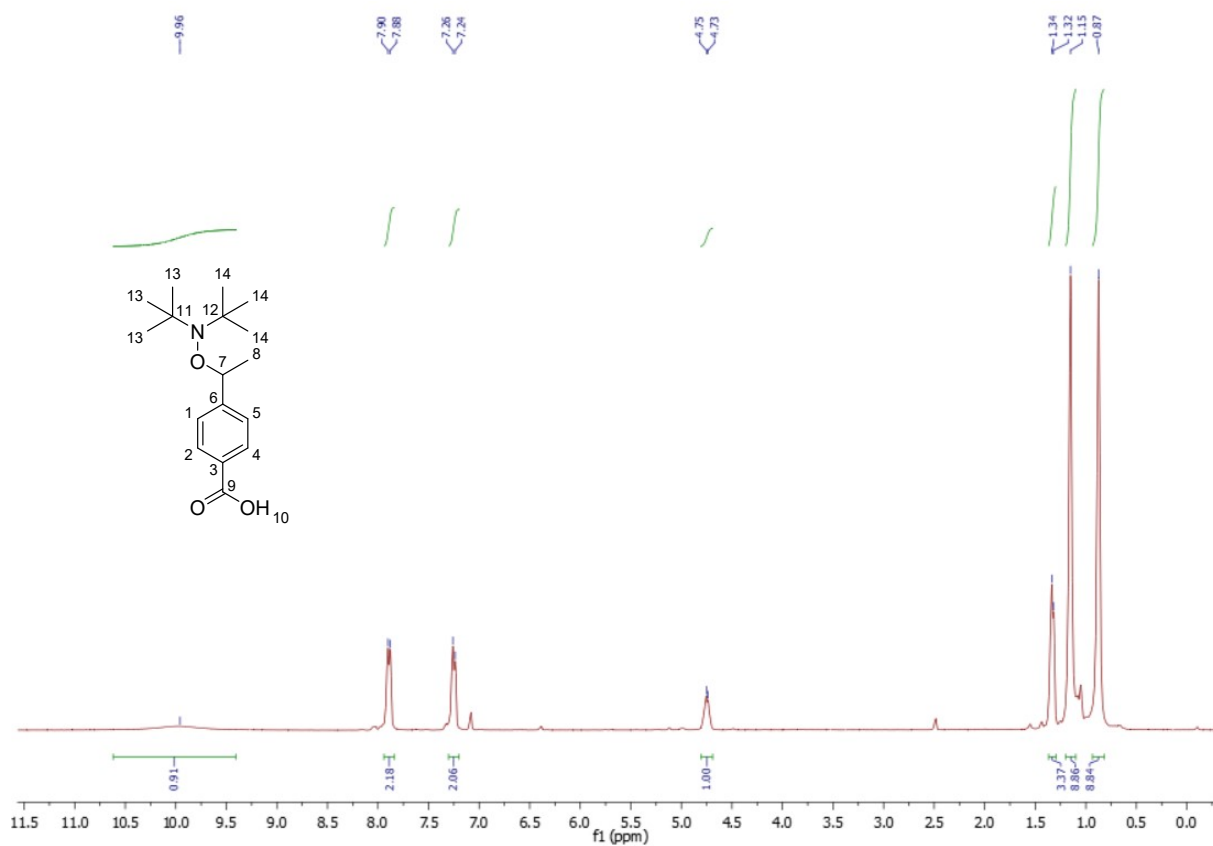


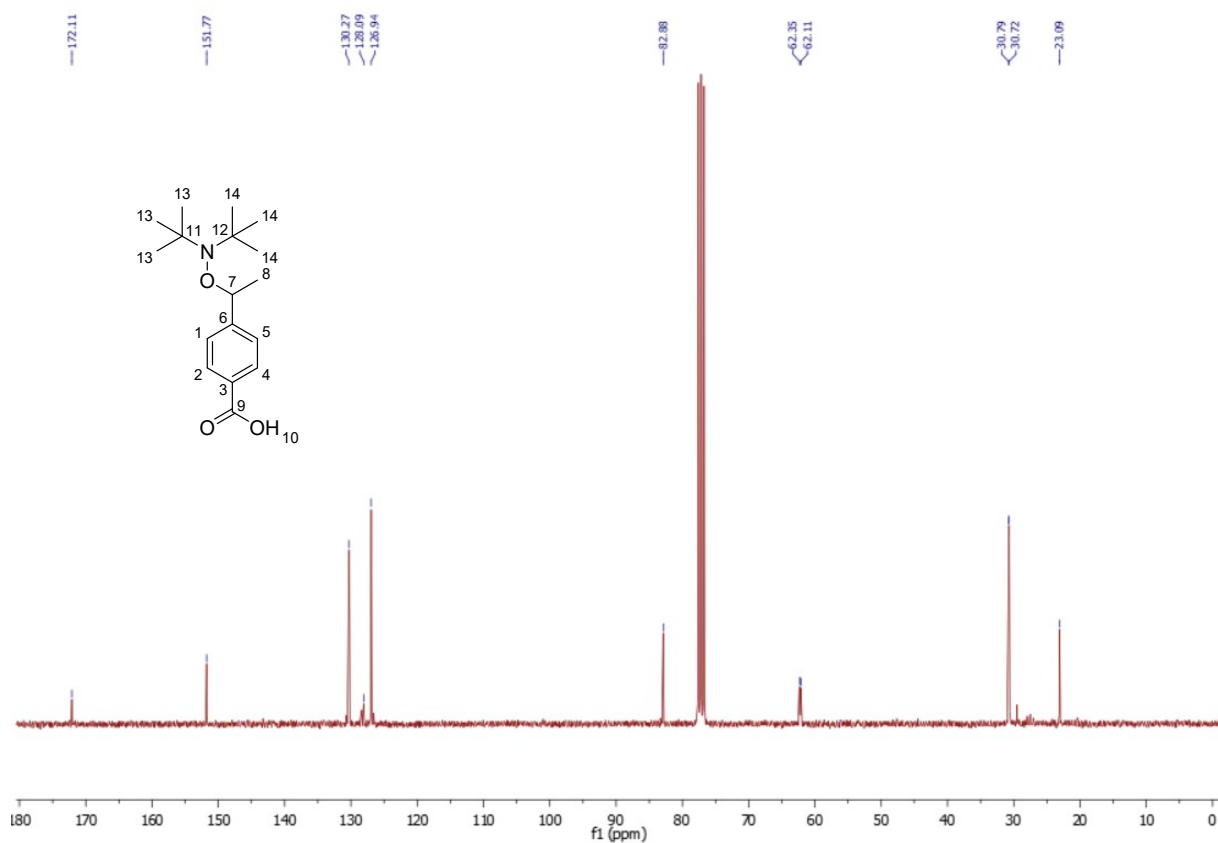
**Figure S1.**  $^1\text{H}$  NMR spectrum of Methyl 4-vinylbenzoate.



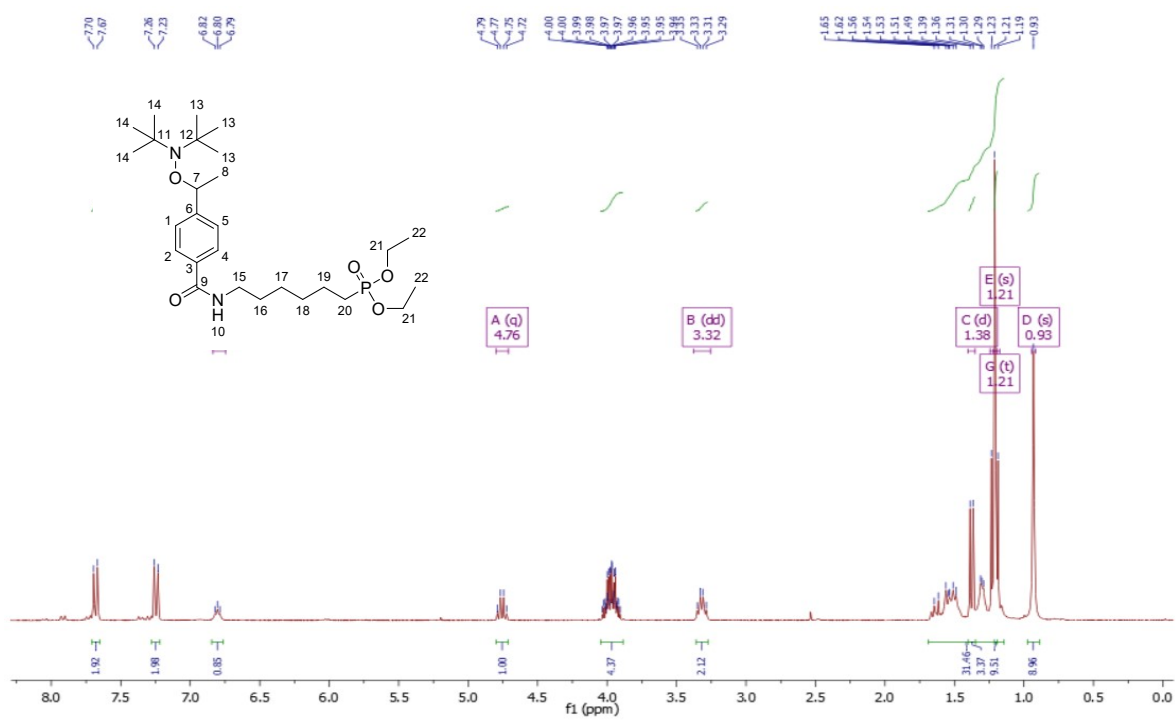


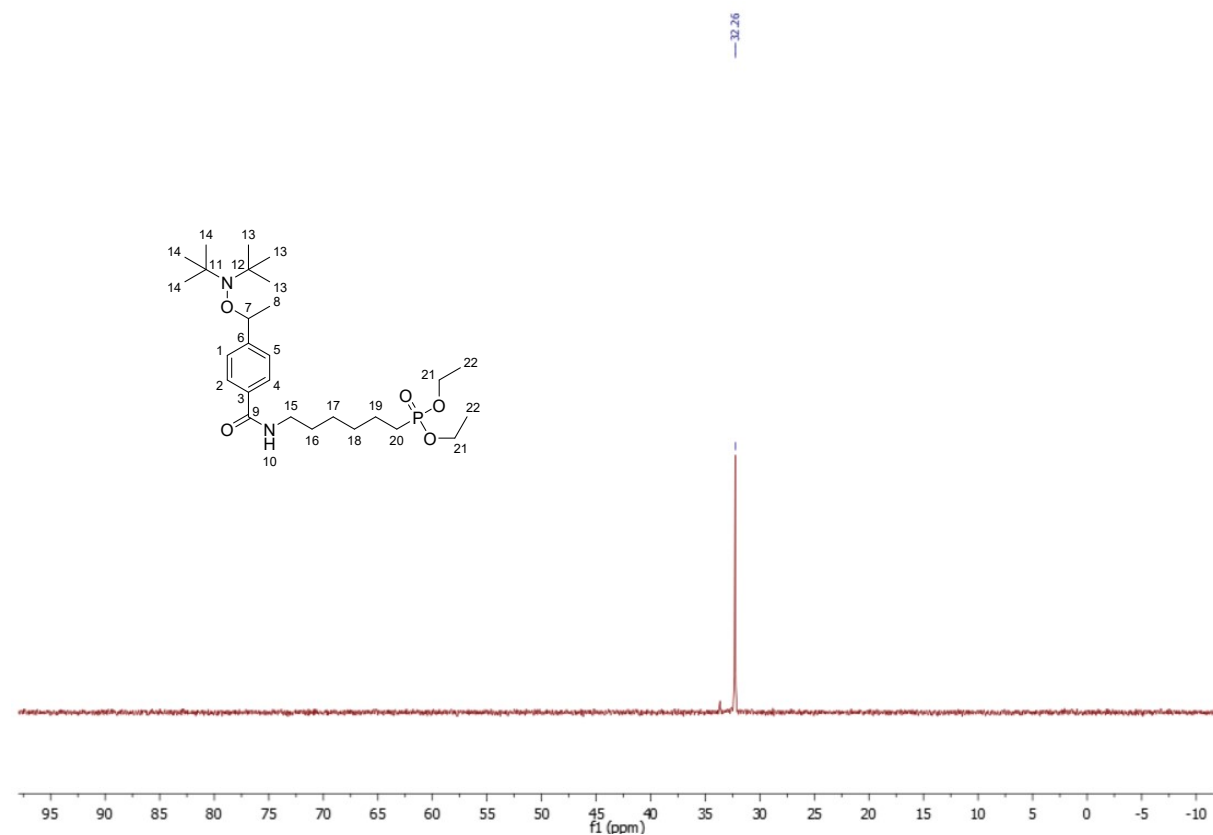
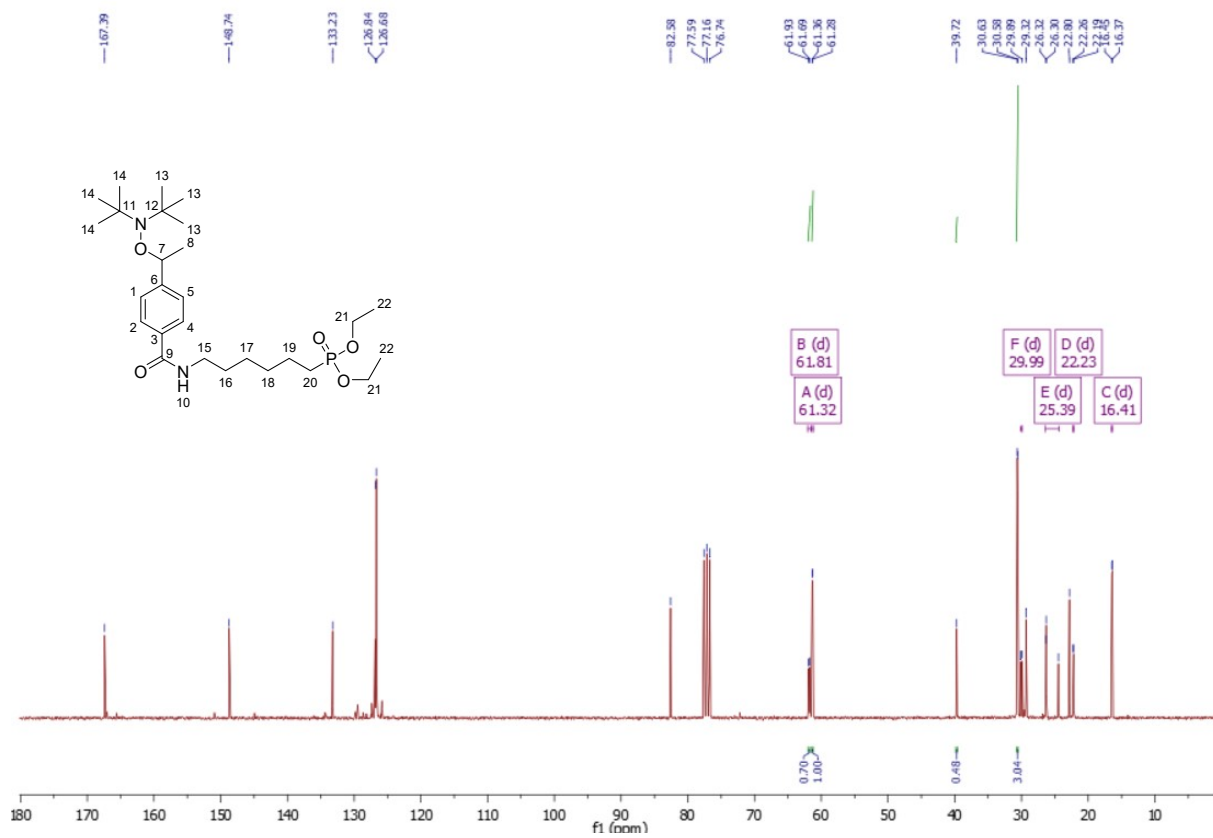
**Figure S2.** <sup>1</sup>H (up) and <sup>13</sup>C (down) NMR spectra of Methyl 4-(1-((di-tert-butylamino)oxy)ethyl)benzoate



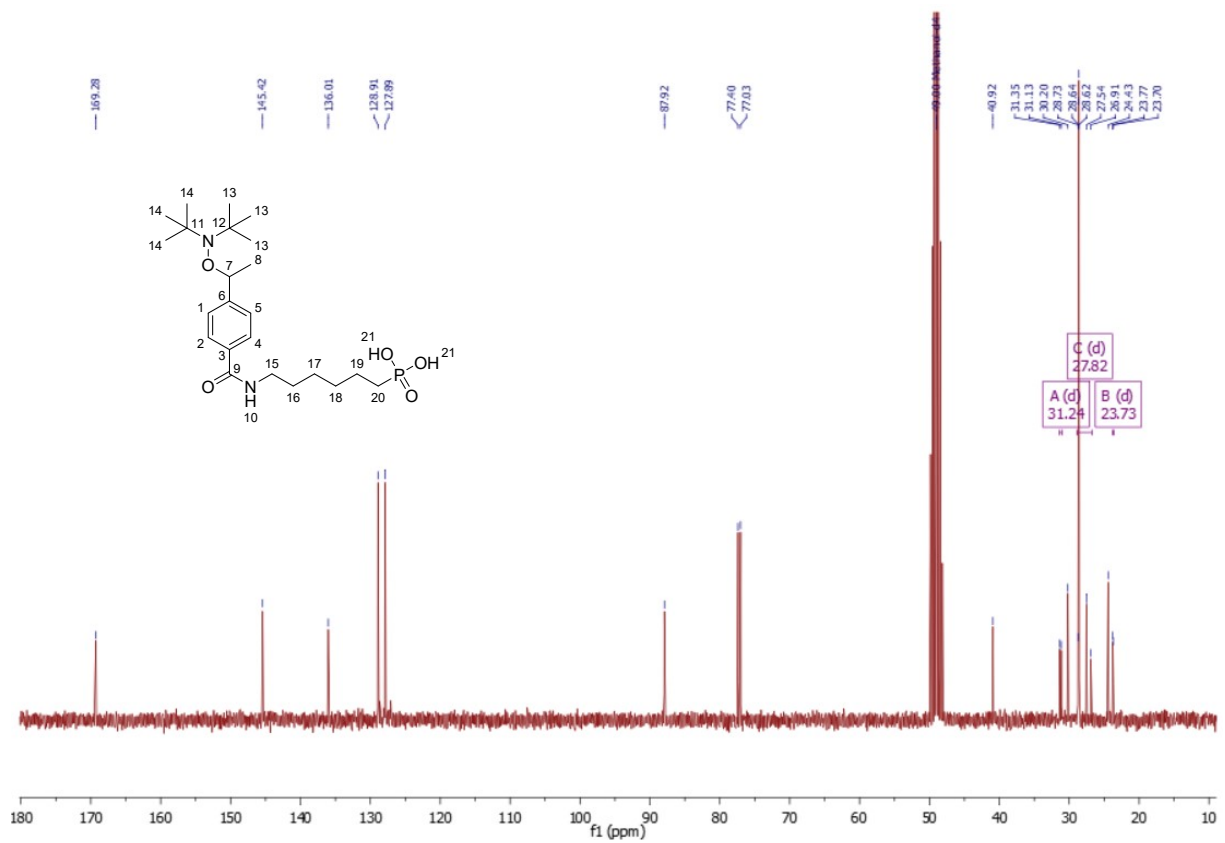
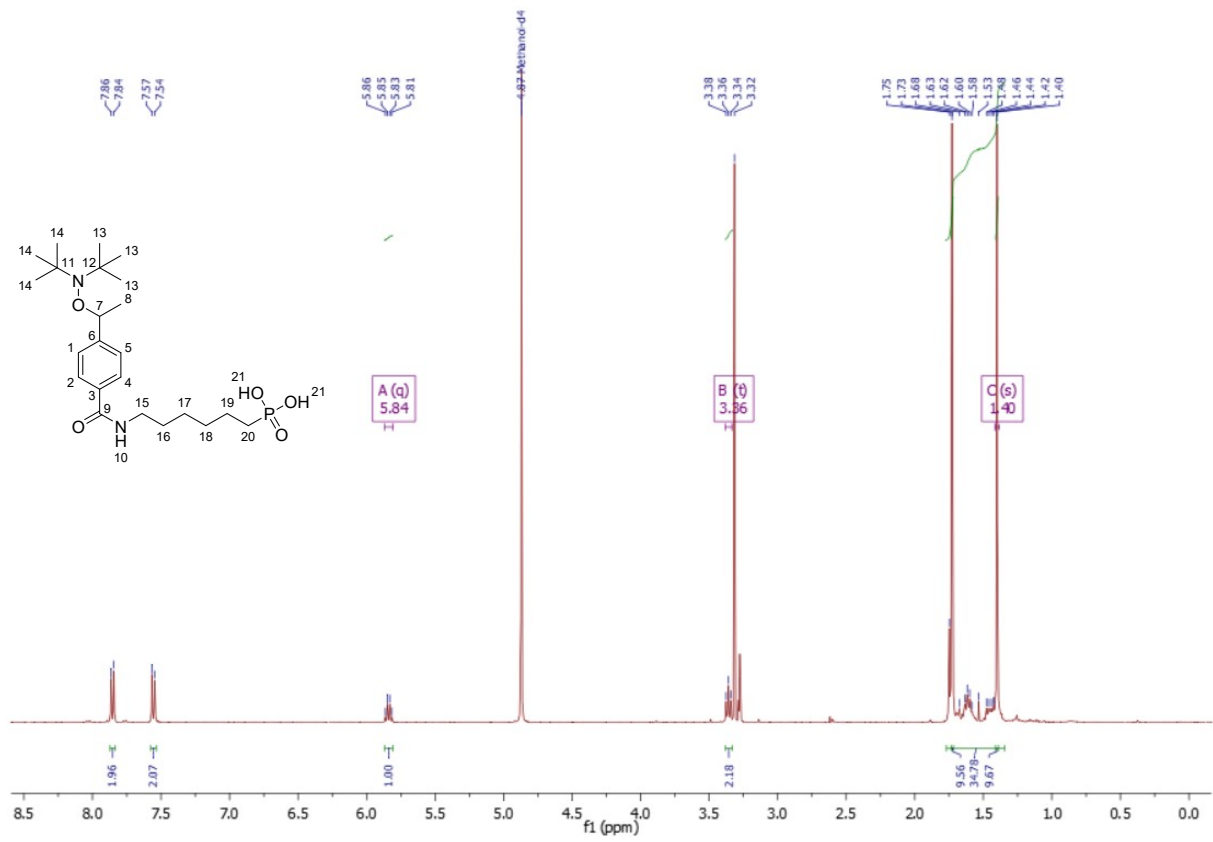


**Figure S3.** <sup>1</sup>H (up) and <sup>13</sup>C (down) NMR spectra of 4-(1-((di-tert-butylamino)oxy)ethyl)benzoic acid.





**Figure S4.**  $^1\text{H}$  (up),  $^{13}\text{C}$  (middle) and  $^{31}\text{P}$  (down) NMR spectra of Diethyl (6-(4-(1-((di-tert butylamino)oxy)ethyl) benzamido) hexyl)phosphonate.



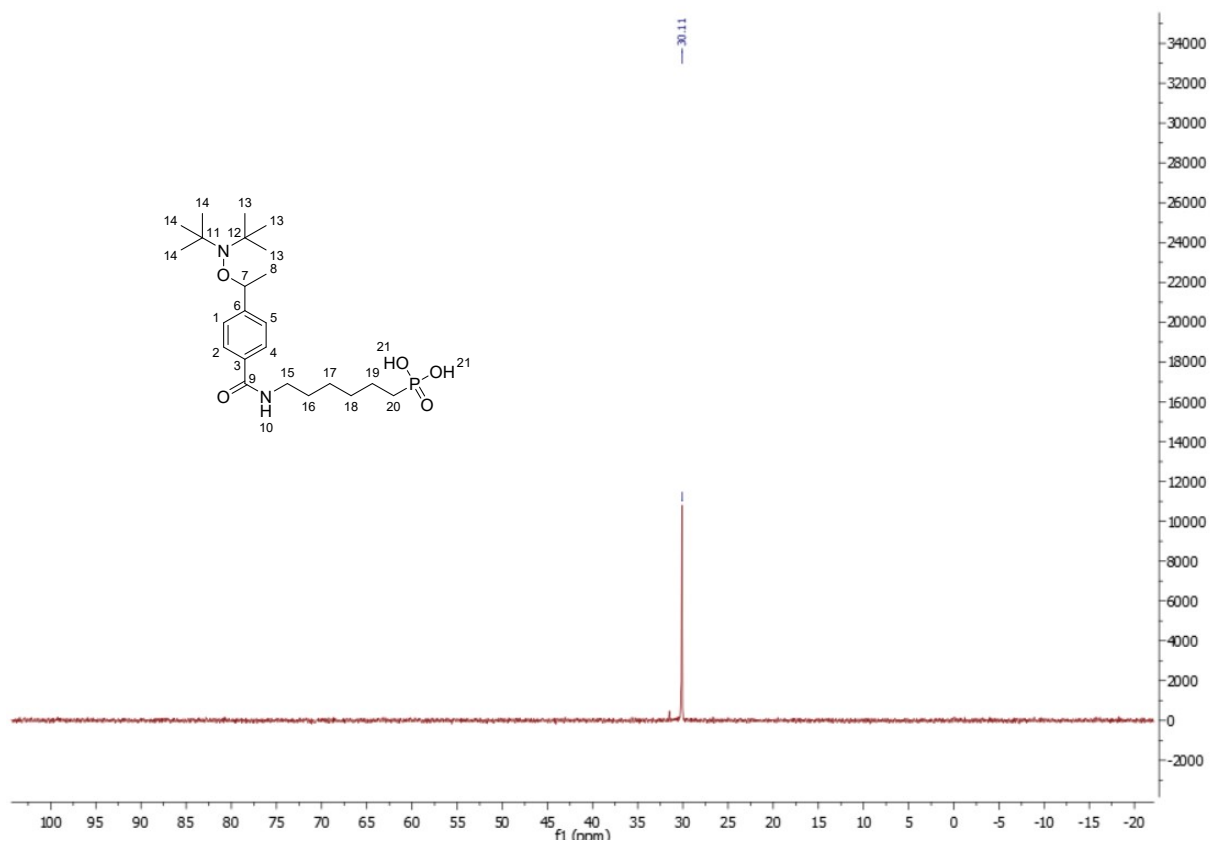


**Figure S5.**  $^1\text{H}$  (up),  $^{13}\text{C}$  (middle) and  $^{31}\text{P}$  (down) NMR spectra of (6-(4-(1-((di-tert-butylamino)oxy)ethyl)benzamido)hexyl) phosphonic acid

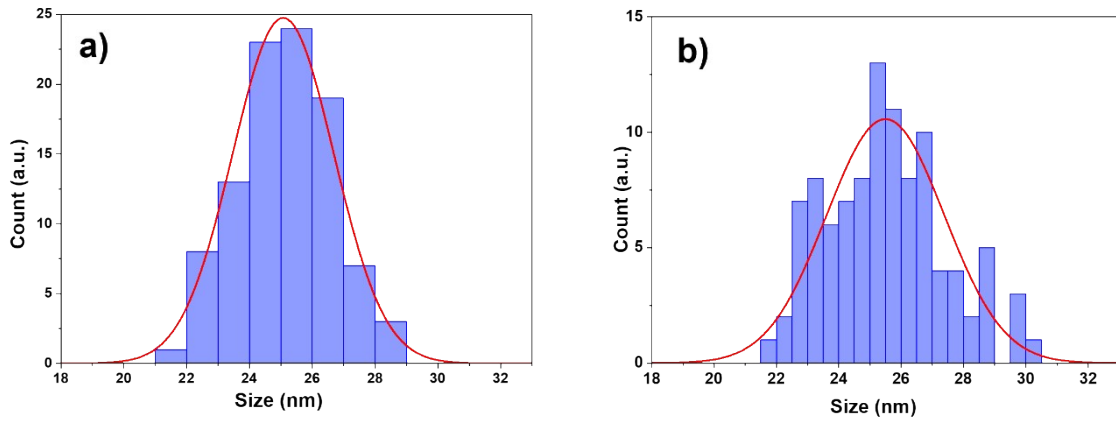


**Figure S6.** Histograms showing the size distributions for: (a) IONP/OA/OL nanoparticles, and (b) IONP@alkoxyamine nanoparticles. The standard normal distribution is represented by the red line.

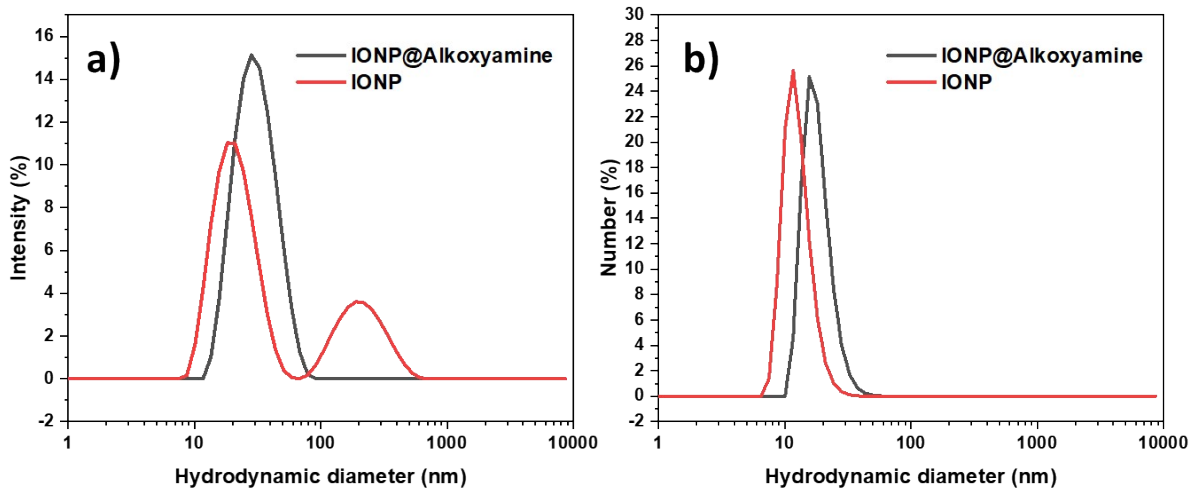


**Figure S7.** Hydrodynamic diameter distribution by intensity (a) and by number (b) for IONP/OA/OA (in red) and IONP@alkoxyamine (in grey) in methanol.

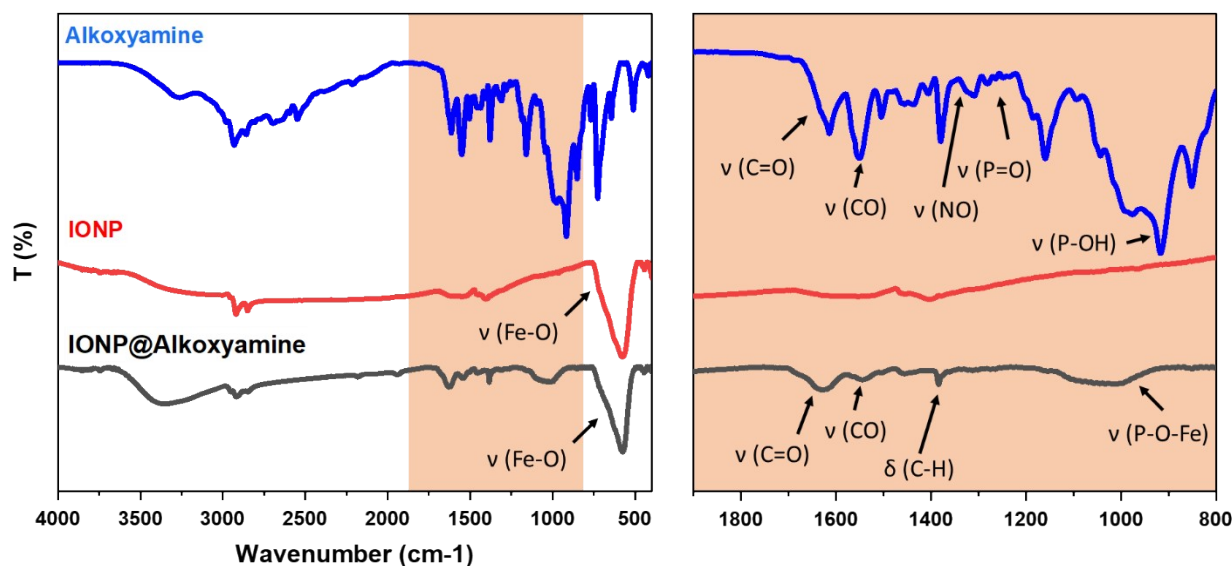


**Figure S8.** Infrared spectra for the pristine IONP (in red), IONP@alkoxyamine (in grey), and free alkoxyamine molecule, ((6-(4-(1-((di-tert-butylamino)oxy)ethyl) benzamido)hexyl)phosphonic acid) (in blue).

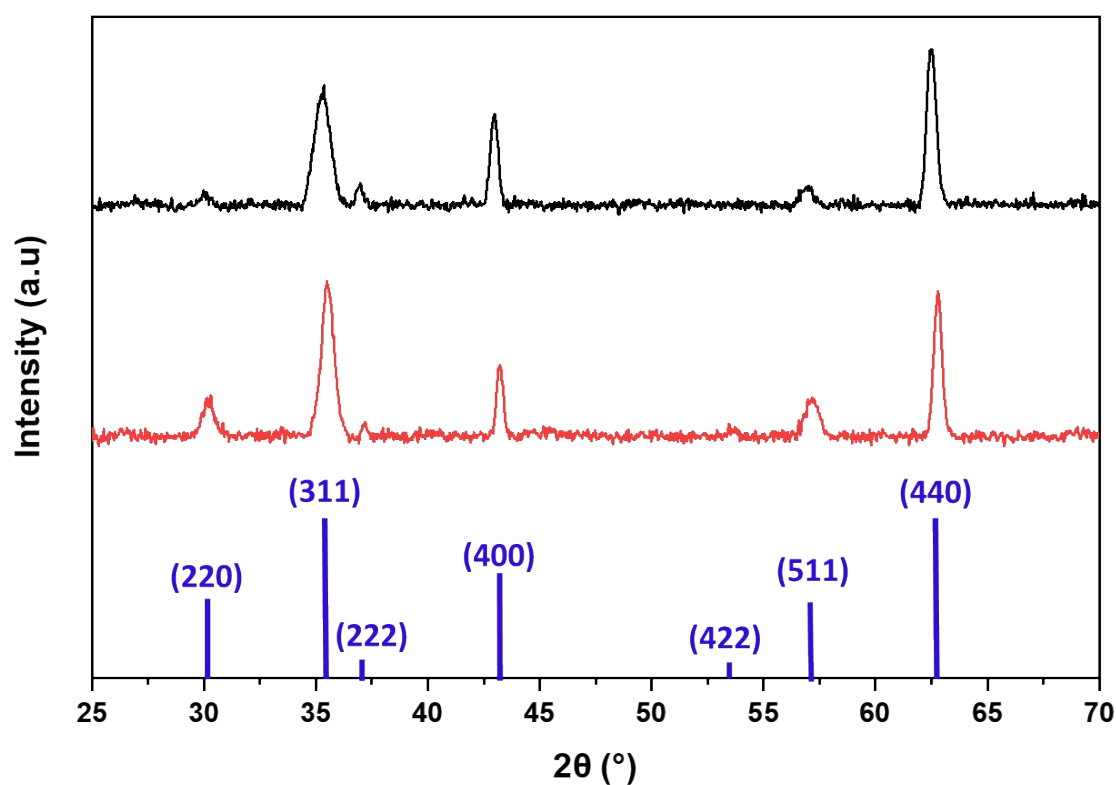


**Figure S9.** XRD pattern of naked IONP (red) and IONP@alkoxyamine (black) powder and reference diffraction peaks corresponding to  $\text{Fe}_3\text{O}_4$

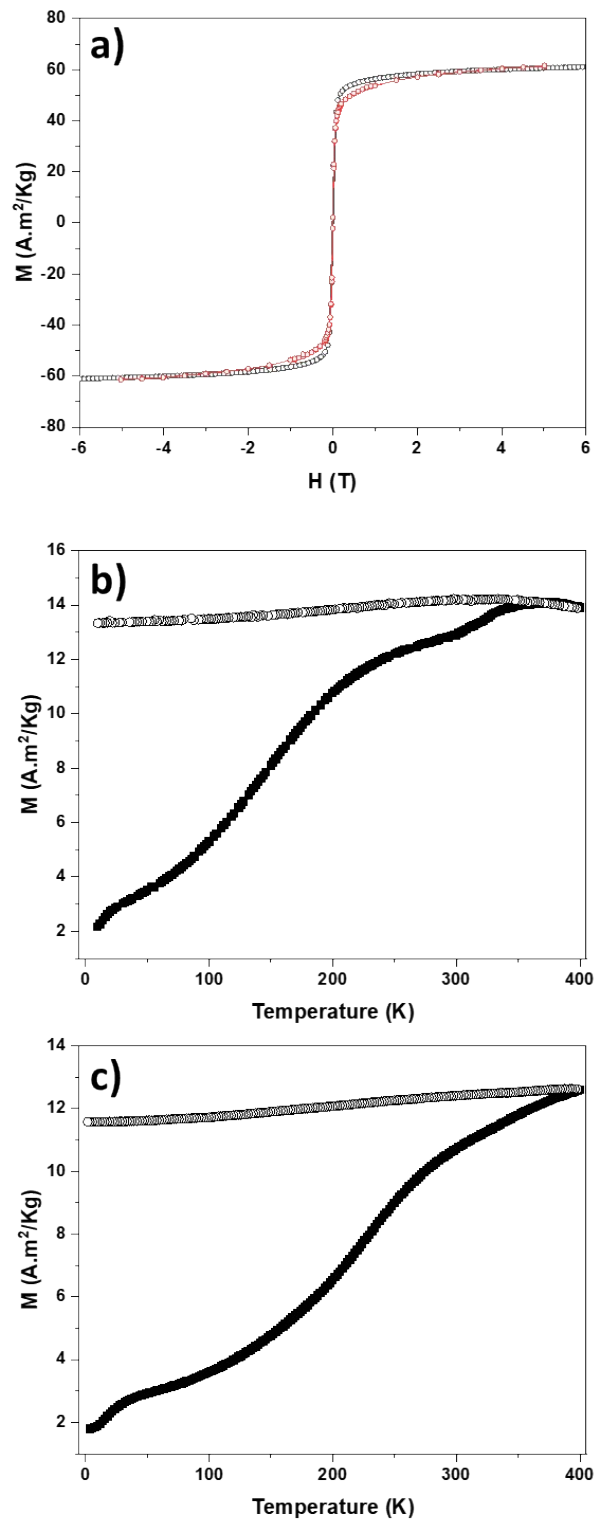


**Figure S10.** (a) Hysteresis loops performed for the pristine IONP (red squares) and IONP@alkoxyamine nanoparticles (black squares) at 300 K between -6 and 6 T. Temperature dependence of the magnetization performed in the FC (open symbols)-ZFC mode (full symbols) for the pristine IONP (b) and for IONP@alkoxyamine nanoparticles (c) measured under an applied dc magnetic field of 100 Oe.

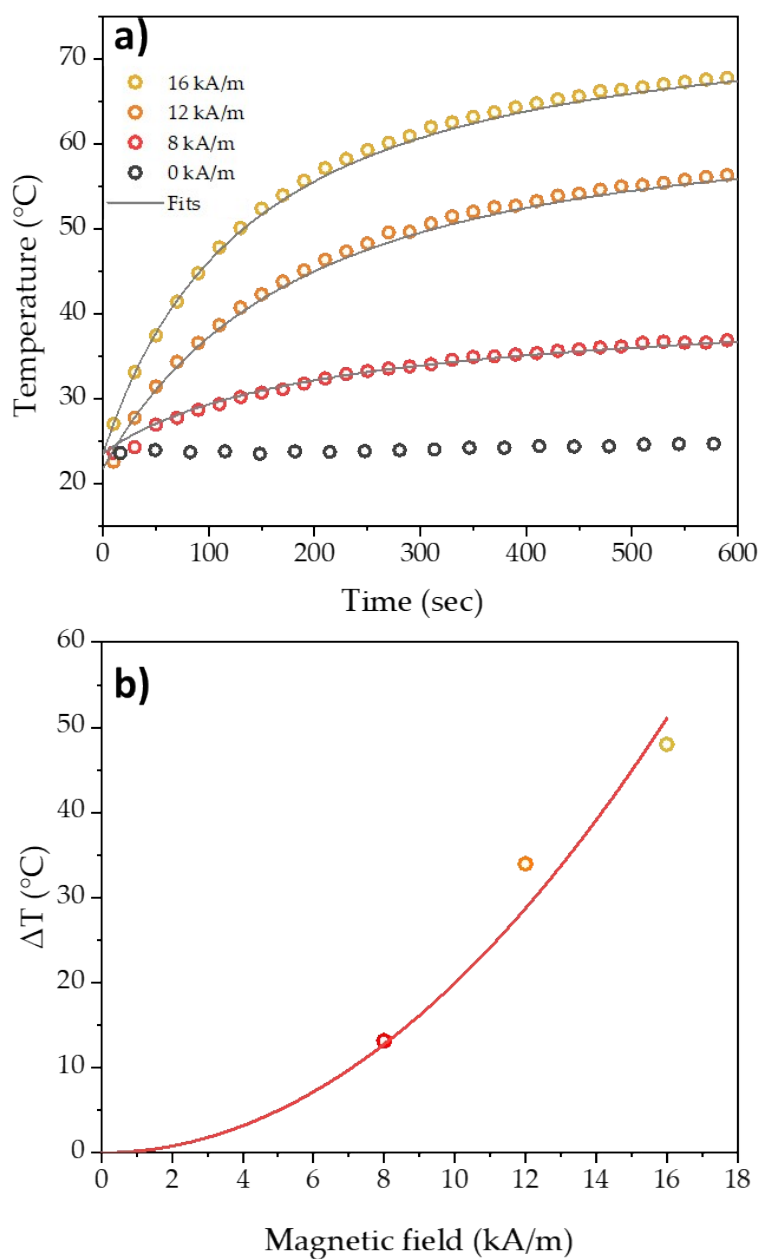


**Figure S11.** a) Magnetothermia experiments performed for IONP@alkoxyamine colloidal solution of  $2.9 \text{ mg mL}^{-1}$  in tert-butylbenzene under different AMF (340 kHz), b)  $\Delta T$  vs magnetic field for IONP@alkoxyamine colloidal solution of  $2.9 \text{ mg mL}^{-1}$  in tert-butylbenzene.

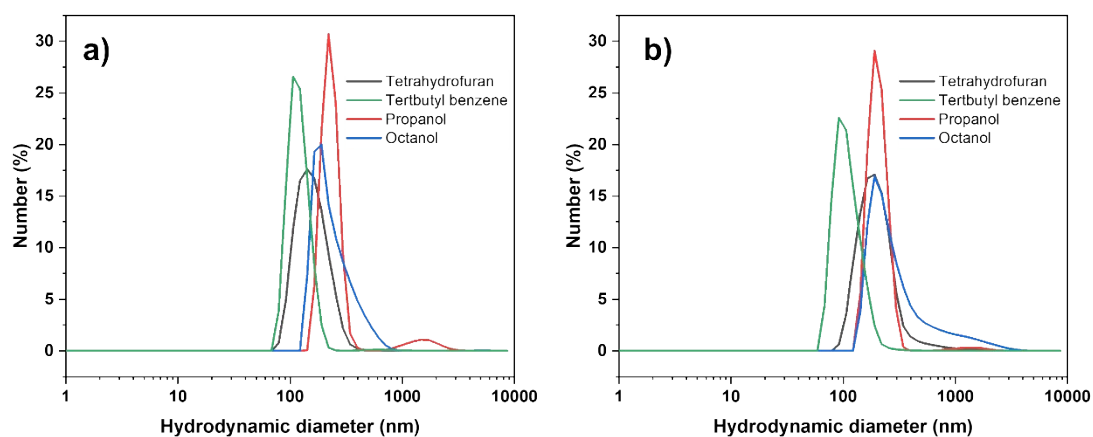


**Figure S12.** Hydrodynamic diameter distribution by number for IONP@alkoxyamine in a series of solvents 10 min (a) and 2h (b) after dispersion.

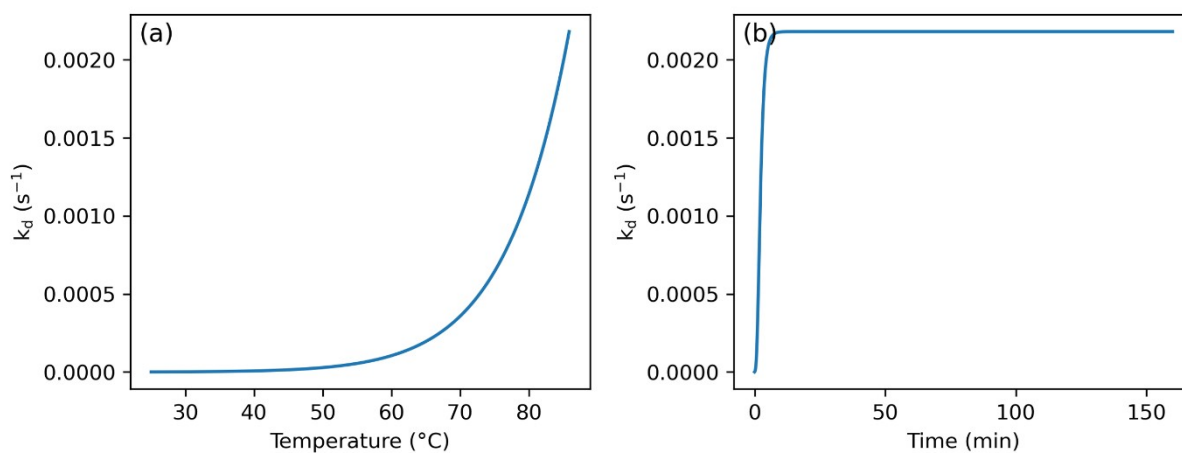


**Figure S13.** a) The  $k_d$  constant as a function of temperature (a) and time (b) used in numerical simulations for IONP@alkoxyamine nanoparticles' homolysis.

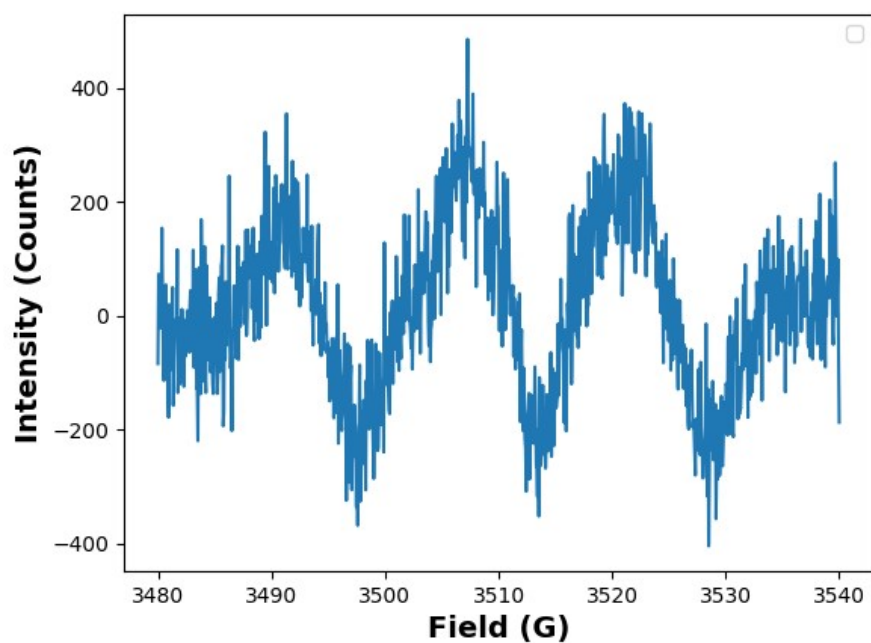


**Figure S14.** EPR spectrum of free alkoxyamine molecule in tert-butylbenzene submitted to laser irradiation at 808 nm (laser power of  $2.6 \text{ W}\cdot\text{cm}^{-2}$ ) during 20 minutes.

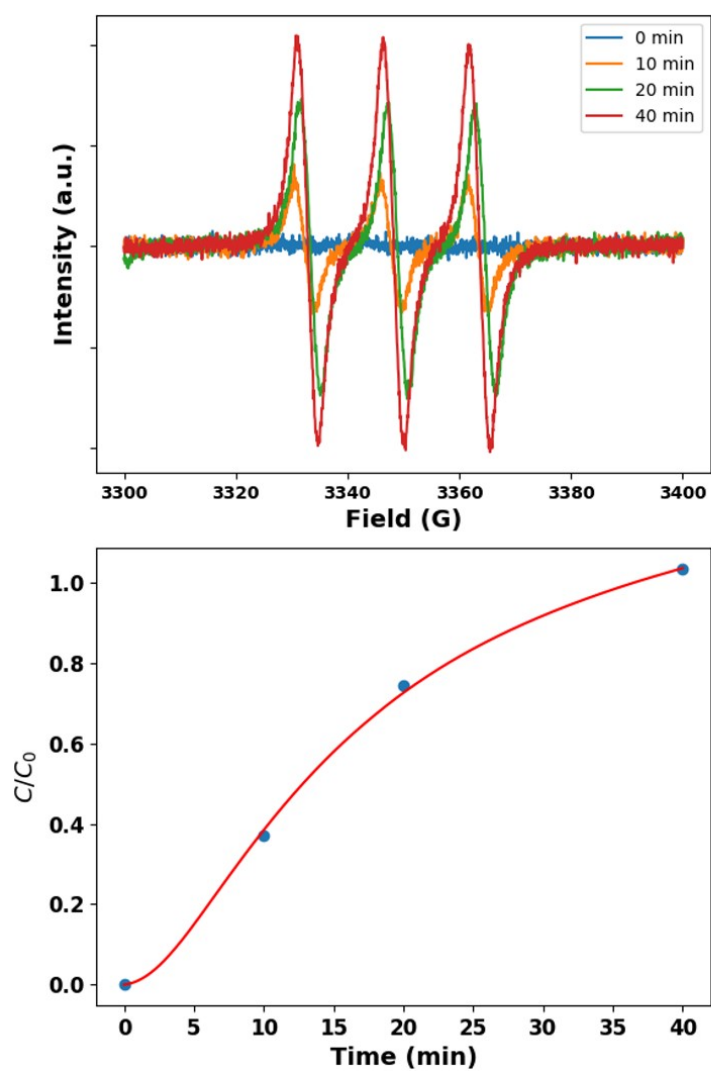


**Figure S15.** (a) EPR spectra for the *tert*-butylbenzene solutions of IONP@alkoxyamine nanoparticles ( $2.9 \text{ mg}\cdot\text{mL}^{-1}$ ) before and after 10, 20 and 40 min after light irradiation at 808 nm ( $2.6 \text{ W}\cdot\text{cm}^{-2}$ ); (b) Homolysis kinetic represented as  $C/C_0$  vs time curve. The red line represents the best fit with the eq. (1):  $k_d = 3.6 \cdot 10^{-2} \text{ s}^{-1}$ ,  $T_{\text{max}} = 109 \pm 6.7 \text{ }^\circ\text{C}$ , macroscopic temperature is of  $50 \text{ }^\circ\text{C}$ .

## Models & theory

### 1. Determination of the Specific Absorption Rate (SAR).

The SAR (in  $W g^{-1}$ ) is defined as follows:

$$SAR_{Fe} = \frac{P}{m_{Fe}} \quad or \quad SAR_{NP} = \frac{P}{m_{NP}} \quad (1)$$

With  $SAR_{Fe}$  and  $SAR_{NP}$  the SAR defined with the mass of Fe ( $m_{Fe}$ ) or the mass of the magnetic nanoparticle (NP) ( $m_{NP}$ ), respectively.  $P$  represents the power produced by the magnetic hyperthermia phenomenon. In this article, we will use  $m_{NP}$  as reference.

Usually, the SAR values are calculated in the adiabatic approximation (no energy exchange between the sample and the environment):

$$P = m_f c_f \cdot \frac{dT}{dt} \quad (2)$$

$$SAR_{NP} = \frac{m_f c_f}{m_{NP}} \cdot \frac{dT}{dt} \quad (3)$$

where  $m_f$  and  $c_f$  are the mass and the weighted heat capacity of the fluid, respectively.

If we want to take into account the possibility of energy exchange between the sample and the environment, we need to rewrite the equation (2). The Newton temperature equation law is a simple phenomenological model, which tends to reproduce the thermal evolution of such case. Equation (2) becomes:

$$m_f c_f \cdot \frac{dT}{dt} = P - h \cdot A \cdot (T - T_0) \quad (4)$$

with  $h$  is a phenomenological term for the energy transfer between the sample and the environment,  $A$  represents the area where the transfer occurs and  $T_0$  is the temperature of the environment.

The solution of the differential equation (4) is:

$$T(t) = \frac{P}{hA} + T_0 - \frac{P}{hA} \cdot \exp\left(-\frac{hA}{m_f c_f} t\right) \quad (5)$$

However, in some cases this phenomenological law cannot be sufficient. More generally, the energy transfer between the sample and the environment can be represented by an unknown function, which depends on  $T$  and  $T_0$ . We will define this function as  $f(T, T_0)$ . Then, equation (2) becomes:

$$m_f c_f \cdot \frac{dT}{dt} = P - f(T, T_0) \quad (6)$$

If we consider that  $T_0$  is fixed and the difference between  $T$  and  $T_0$  is small, then  $f(T, T_0)$  has only one variable  $f(T)$  and can be write using the Taylor series. For order 1 we have:

$$m_f c_f \cdot \frac{dT}{dt} = P - (T - T_0) \frac{\partial f(T_0)}{\partial T} \quad (7)$$

Equation (7) is in fact the Newton equation law, and admits an analytical solution. If equation (7) is not sufficient to reproduce the experimental behavior, we can use the order 2 of the Taylor series of  $f(T)$ :

$$m_f c_f \cdot \frac{dT}{dt} = P - (T - T_0) \frac{\partial f(T_0)}{\partial T} - \frac{(T - T_0)^2 \partial^2 f(T_0)}{2 \partial T^2} \quad (8)$$

This differential equation is more complex. We have chosen to solve this equation numerically, using the finite difference method:

$$T(t + \Delta t) = T(t) + \frac{\Delta t}{m_f c_f} (P - (T(t) - T_0) \cdot A - (T(t) - T_0)^2 \cdot B) \quad (9)$$

$$\text{With, } A = \frac{\partial f(T_0)}{\partial T} \text{ and } B = \frac{1}{2} \frac{\partial^2 f(T_0)}{\partial T^2}.$$

It is interesting to note that:

$$m_f c_f = \frac{m_{NP} \cdot c_{V,f}}{C_{NP}} \quad (10)$$

with  $m_{NP}$ ,  $c_{V,f}$  and  $C_{NP}$  are the mass of the nanoparticles, the volume heat capacity of the fluid and the concentration of nanoparticles, respectively.

Equations (7) and (8) were used to fit the experimental data shown on Figures 3, S11, S12. The extracted  $SAR_{NP}$  from equation (7) and (8) are equal to  $259 \pm 1$  W/g and  $420 \pm 1$  W/g, respectively. The value of  $420 \pm 1$  W/g will be held since the equation (8) provides the best fit. The parameters used for these fits are  $C_{NP} = 4$  mg mL<sup>-1</sup> and  $c_{V,f} = 1.538$  J.mL<sup>-1</sup>.K<sup>-1</sup>.

The ILP may be calculated as:

$$ILP = \frac{SAR}{f \cdot H^2} \quad (10)$$

## 2. Fits for the $\Delta T$ as a function of the concentration curve for magneto- and photothermia experiment

The simplify heat equation for a magneto- or photothermal can be write as follows:

$$m_f c_f \cdot \frac{dT}{dt} = P - h \cdot (T - T_0) \quad (11)$$

where  $m_f$  and  $c_f$  are the mass and the weighted heat capacity of the fluid, respectively. The term  $h$  represents the energy exchange rate between the liquid and the environment.  $P$  represents the thermal power source, which is produced by the conversion of magnetic or light energy.

The term  $\Delta T$  represents the difference between the initial temperature and the stabilized temperature when  $T$  reaches the plateau at  $t \rightarrow \infty$ . The plateau at  $t \rightarrow \infty$  means that  $dT(t \rightarrow \infty)/dt = 0$ . Then if we call  $T_\infty$  the temperature reached on the plateau we have:

$$P - h \cdot (T_\infty - T_0) = 0 \quad (12)$$

and so:

$$\Delta T = \frac{P}{h} \quad (13)$$

In the case of magnetothermia,  $P$  is directly proportional to the quantity of nanoparticles in the solution, due to the deep penetration of the magnetic field inside the solution. That means the variation of  $\Delta T$  as a function of the nanoparticle concentration is linear.

In the context of photothermia, the absorption of light by the entire solution is observed to exhibit a nonlinear dependence on the concentration of nanoparticles. Considering a laser beam with a direction along the x-axis. The power intensity of the beam at the position  $x$  in the solution is defined by:

$$P_{beam}(x) = P_{laser} \cdot \exp(-a \cdot x) \quad (14)$$

with  $a$  the absorption coefficient, and  $P_{laser}$  the output power of the laser.

The total absorbed power after the light has traversed a distance of  $d$  is given by the following equation:

$$P_{abs} = P_{laser} - P_{beam}(d) \quad (15)$$

If we develop, we have:

$$P_{abs} = P_{laser} \cdot (1 - \exp(-a \cdot d)) \quad (16)$$

The heat source power, as expressed in Equation (13), is proportional to the absolute pressure,  $P_{abs}$ , as demonstrated by the following relationship:

$$P = P_{abs} \cdot \eta \quad (17)$$

with  $\eta$  the light to heat conversion coefficient.

If we make the classical approximation that the coefficient absorption  $a$  is proportional to the nanoparticle concentration then we have:

$$a = \alpha \cdot c_{NP} \quad (18)$$

with  $\alpha$  the concentration normalized coefficient absorption, and  $c_{NP}$  the concentration in mg/mL of nanoparticles in the solution.

Then, from the previous equations, we can deduce the variation of  $\Delta T$  as a function of the nanoparticle concentration for a photothermal experiment.

$$\Delta T = \frac{\eta}{h} P_{laser} \cdot (1 - \exp(-\alpha \cdot d \cdot c_{NP})) \quad (19)$$

### 3. Investigation of the homolysis kinetic of the radical release by EPR

A suspension of IONP@alkoxyamine nanoparticles **3** ( $10^{-3}$  M) in *tert*-butylbenzene was submitted to the action of an ac magnetic field ( $\approx 20$  mT at a frequency of 350 kHz). At each timepoint, 100  $\mu$ L was withdrawn and cooled in an ice bath to stop the reaction. After magnetic separation, 50  $\mu$ L of the supernatant was analysed by EPR.

A correlation between intensities measured by EPR and concentrations of alkoxyamines was performed using a calibration at three concentrations ( $10^{-4}$  M,  $10^{-5}$  M, and  $10^{-6}$  M) of alkoxyamine in *tert*-butylbenzene, in order to obtain an intensity value ( $I_{ref}$ ) for a reference concentration ( $C_{ref}$ ). Those solutions had been incubated at 120  $^{\circ}$ C overnight and measured by RPE. From each supernatant analysed during the kinetic study, the intensity of the first peak is measured, and the conversion rate in radicals was estimated using this following equation:

$$\frac{C}{C_0} = \frac{I \times C_{ref}}{C_0 \times I_{ref}}$$

with  $C_0 = 1$  mM is the initial concentration, and  $I$  is the intensity of the first peak measured by EPR at each timepoint. When plotted as a function of time, the kinetic constant  $k_d$  can be determined with the slope of the linear regression. The temperature at the surface of the nanoparticles can be estimated by using the Arrhenius law:

$$k_d = A \times \exp(-E_a/RT) \text{ and}$$

$$T = \frac{-E_a}{R \cdot \ln\left(\frac{k_d}{A}\right)}$$

where  $E_a$  is the activation energy,  $A = 2.4 \cdot 10^{14} \text{ s}^{-1}$  is the pre-exponential factor in the case of the alkoxyamine homolysis,  $R$  is the perfect gas constant and  $k_d$  is a homolysis constant.